Nickel Formate Route to the Growth of Carbon Nanotubes

Junfeng Geng, Hongwei Li, Vladimir B. Golovko, Douglas S. Shephard, David A. Jefferson, and Brian F. G. Johnson*

Department of Chemistry, Cambridge University, Lensfield Road, Cambridge CB2 1EW, U.K.

Stephan Hofmann, Britta Kleinsorge, and John Robertson

Department of Engineering, Cambridge University, Trumpington Street, Cambridge CB2 1PZ, U.K.

Caterina Ducati

Department of Materials Science and Metallergy, Cambridge University, Pembroke Street, CB4 3QZ, U.K.

Received: May 17, 2004

Nickel formate serves as an ideal catalyst precursor for surface-bound thermal and plasma-enhanced CVD growth of carbon nanotubes. As the method of deposition of the Ni catalyst is solution-based, it benefits from a low-cost, large-area growth, ease of operation and suitability for coating substrates with complex shapes and structures.

Introduction

Carbon nanotubes (CNTs) have been considered as ideal candidates for many applications due to their unique atomic structure, an inherent small tip radius, high surface area and aspect ratio, excellent chemical inertness and mechanical strength.[1,2]

Among the many growth techniques, chemical vapor deposition (CVD) or plasma-enhanced chemical vapor deposition (PECVD) offer controlled surface-bound growth on flat substrates.[3,4] In a CVD-based process, catalyst and catalyst preparations are essential because the growth occurs at the interface of the catalyst and the hydrocarbon vapor.[5] Hence, formation of an active, uniform catalyst layer is a critical step in a successful surface-bound CVD process.

Deposition of catalyst may be realized by a physical method, as for example, using thermal evaporation or magnetron sputtering to generate a homogeneous thin metal film, which in a subsequent growth step, breaks into small metal islands as catalyst.[6,7] Although physical methods have proven very effective, they require a vacuum facility to process catalyst deposition, and in general, are not suitable for coating a substrate with complex shapes. Alternatively, a chemical method may be used, as for example, introducing metal colloidal nanoparticles (Fe, Co, and Ni) to the catalyst.[8,9] Metal colloidal nanoparticles may be pre-controlled in a narrow size distribution in either the synthesis process or using an after-process technique for size selection. However, the colloids are frequently air-sensitive, making their manipulation difficult and, to some extent, limiting the large-scale production of carbon nanotubes. Another commonly used method is through a catalyst precursor, such as an inorganic or organometallic salt, leading to the desired metal nanoparticles by the thermal decomposition of the precursor at high temperatures.[10,11] The precursor method takes advantages of low-cost, good stability in air, ease of operation and commercially available starting materials. It is also suitable for coating 3D substrates with complex shapes and structures.

We have found that nickel formate may serve as an ideal catalyst precursor for formation of the desired Ni nanoparticles for growth of carbon nanotubes. In our previous report, we demonstrated that using this compound, high-purity single-wall carbon nanotubes were produced in high yield.[12] In fact, nickel formate may be used not only for single-wall nanotubes but also for versatile growth of carbon nanotubes with varied structures. In this paper, we wish to address the issue of why nickel formate is such an ideal catalyst precursor on one hand, and to demonstrate surface-bound growth of multiwalled carbon nanotubes on the other. The choice of the surface growth on the flat SiO_2/Si substrate is based on a common recognition that such grown nanotubes are potentially significant in microelectronic applications, such as for electron field emission, flat panel display and supercapacitors.[13−15]

Experimental Section

Deposition of the Catalyst. For deposition of the nickel catalyst, silicon wafer was first cleaned by ethanol and acetone in an ultrasonic bath and rinsed with distilled water. Nickel formate dihydrate was purchased from Degussa, as a fine green powder. Deposition of the catalyst was carried out by simply casting a drop of the aqueous or methanol solution of nickel formate onto the substrate. The samples were then left to dry in air. The concentration of the solution may be varied, according to the growth purpose and catalyst loading. A typical concentration falls in the range 5×10^{-3} to 2.2×10^{-2} M. The thickness of the formate film depends on the amount of solution on the surface. To keep the film uniform, a trace amount of anionic surfactant, such as lauric acid, may be mixed into the solution. The Ni nanoparticles were formed in situ by thermal decomposition of the formate precursor in the CNTs growth process.

Growth of the Carbon Nanotubes. The growth methods are basically the same as described previously.[7,15] In brief, a stainless steel vacuum chamber was used with a base pressure below 10^{-6} mbar. A 20 nm thick SiO_2 layer was grown by thermal oxidation or low-temperature electron cyclotron resonance (ECR) onto a polished n-type Si(100) substrate. The samples were normally heated for 15 min to reach the desired temperatures using a resistively heated graphite stage. For the plasma-enhanced growth, samples with freshly deposited catalyst

* Corresponding author. E-mail: bfgj1@cam.ac.uk.

10.1021/jp047898p CCC: $27.50
Published on Web 11/06/2004

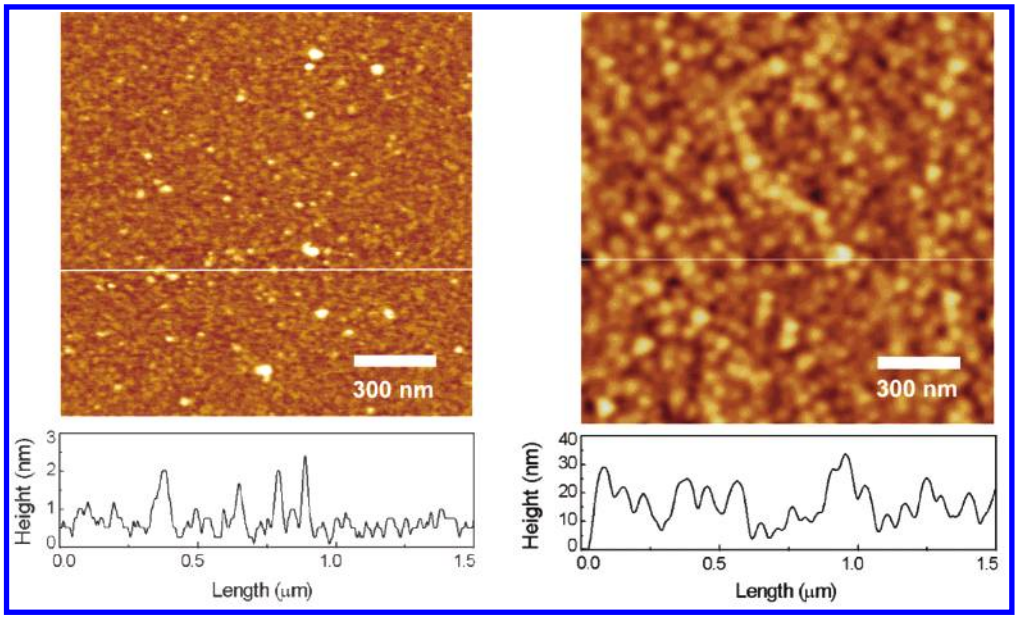

Figure 1. (Upper left): image of the Ni nanoparticles on the surface of silicon substrate under AFM. The particles are formed from thermal decomposition of nickel formate precursor at 500 °C. The employed solution of the precursor has a concentration of 5×10^{-3} M. AFM operation was carried out by a tapping mode. (Lower left): topographical height measurements for the selected nanoparticles cross-lined in the upper image, showing the typical sizes of the particles. (Upper right): AFM image of the larger and denser Ni nanoparticles formed at identical decomposition conditions but deposited from a higher concentration of the precursor solution (2.2×10^{-2} M). The solution also contains a trace amount of lauric acid. (Lower right): AFM topographical height data showing the typical particle size and size distribution.

precursor were first heated typically to 460 °C in 1.1 mbar of NH_3 (100 sccm). A voltage of 800 V between the sample heater and the gas inlet was employed to generate the dc discharge current. The feed gas, acetylene (C_2H_2, grade 1.5, 55 sccm) was introduced into the chamber as the carbon feedstock immediately after the discharge started. Growth normally lasted 20 min. The C_2H_2/NH_3 ratio and the total pressure were varied from one growth to another depending on growth purpose. A stable discharge of typically 20−40 mA was maintained for a given deposition.

Characterization. After growth, SEM observations were carried out using a JEOL 6340-FESEM system operated at 5 kV. The TEM was performed on a JEOL JEM-3010x operated at 300 kV. The TEM sample was prepared by scratching the tubes off the substrate and then dispersed into toluene assisted by ultrasonication. A drop of such prepared solution was cast onto a holey carbon film on a copper grid for the examination. The Raman studies were performed using a microspectrometer with an incident Ar ion laser at $\lambda = 514.5$ nm and the Renishaw software. Atomic force spectroscopy (AFM) images were obtained by the tapping mode using a Digital Instrument with a nanoscope dimension 3100 controller.

Results and Discussion

Formation of the Ni Nanoparticles. In the solid state, nickel formate typically exists in the form of a dihydrate, $Ni(HCOO)_2 \cdot 2H_2O$. Our measurements using thermal gravimetric analysis (TGA) indicate that the dihydrate loses the crystallized water at a temperature of ca. 160 °C and thermally decomposes between 230 °C and 260 °C, which is consistent with literature reports using TGA analysis[17] and the differential scanning calorimetry (DSC) measurements.[18]

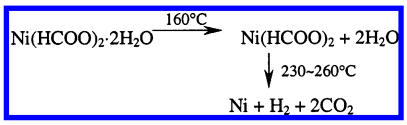

In the presence of hydrogen, the decomposition temperature falls to 180−200 °C.[16] Unlike many other nickel precursors, nickel formate decomposes directly to metallic Ni particles and gas species (H_2, H_2O, CO, and CO_2) without forming the oxide (NiO) intermediate in a vacuum or a gas flow system. This is attributed to a self-redox reaction in which a nickel atom obtains two electrons to be reduced to the metallic state, whereas the two ligands lose two electrons to be oxidized into gaseous species. This excellent characteristic distinguishes nickel formate from other nickel precursors and makes the normally required reducing agents such as H_2 no longer necessary in the formation of phase-pure metallic nickel.[16−18]

It has been established that the catalytic properties of nickel strongly depend on the size of the particles. In our previous report on the growth of single-wall carbon nanotubes,[12] the nearly monodispersed Ni nanoparticles are extremely small, with a typical size of ∼1.0 nm. In that case, the small metal particles result from the well-dispersed nickel formate precursor in the fine and mesoporous silica powder. As to the flat SiO_2/Si substrate, however, we find that Ni particles may be formed in a large-size scope, typically between 1 and 30 nm, depending on experimental conditions. Under the appropriate conditions, a specific particle size with narrow size distribution may be obtained. This has been confirmed by the atomic force spectroscopy (AFM) measurements and from the results of the nanotubes growth.

Figure 1a shows the AFM topographical image of small and discrete Ni nanoparticles prepared by annealing the silicon substrate coated with a thin layer of nickel formate. The calcination was conducted at 500 °C, for 2 min and under an argon atmospheric pressure. As usual for any AFM operation, the accurate particle sizes are measured from their topographic heights. Some typical heights are shown in Figure 1a. In this case, the Ni particles are extremely small, with a typical size between 1 and 2 nm. These particularly small metal particles may be used as ideal catalytic seeds in the growth of single-wall carbon nanotubes. In contrast, Figure 1b shows larger and

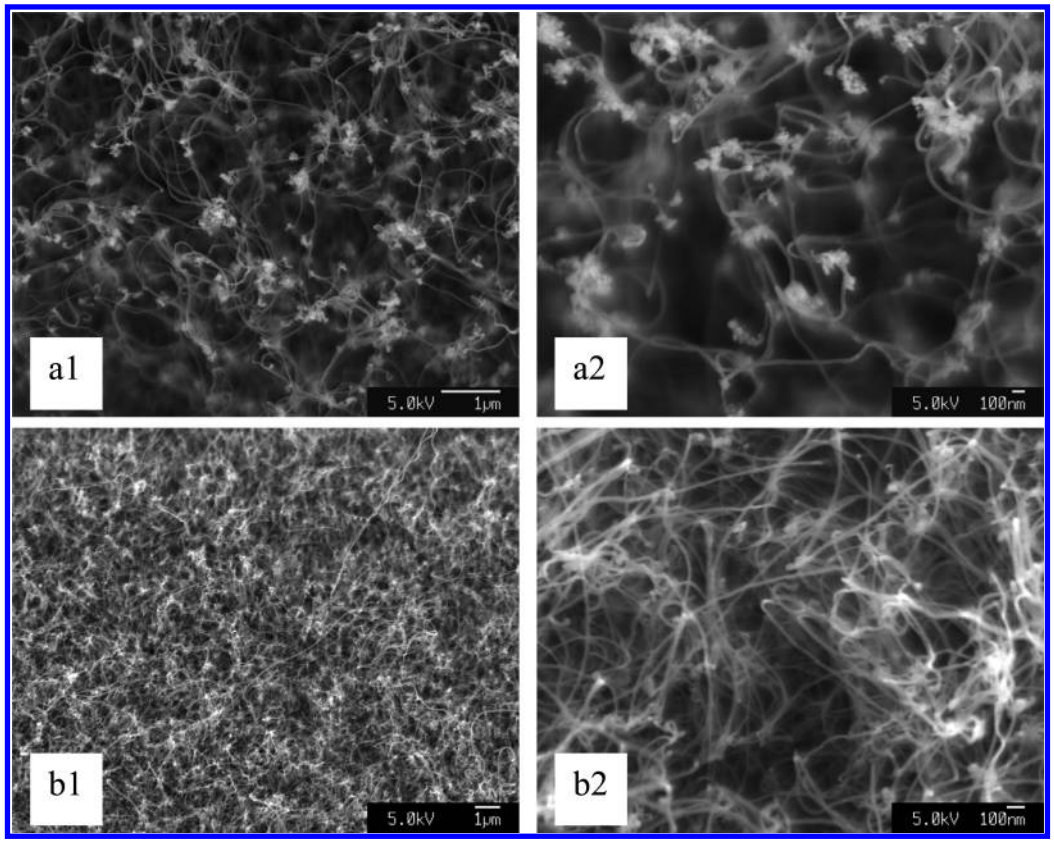

Figure 2. SEM images showing growth behavior of the carbon nanotubes with different catalyst densities on the SiO_2/Si substrate: a1, nanotubes grown from a low surface coverage of the Ni nanoparticles; a2, image of the same sample at a higher magnification; b1, nanotubes grown from identical CVD conditions as those shown in (a) but with a higher catalyst density on the surface; b2, image of the sample b1 at a higher microscope magnification. The CVD growth was performed at 530 °C with NH_3 at 100 sccm, C_2H_2 at 55 sccm, and a total pressure of 60 mbar.

denser Ni particles produced from a higher concentration of the solution (see the figure caption for deposition conditions). The topographic height profile indicates that the particles are fairly uniform, with a typical size of about 20 nm and a size distribution from 15 to 30 nm. Note that (a) and (b) of Figure 1 may represent two extreme examples of the prepared Ni nanoparticles with respect to the particle size. We find that the particles with a size between these two extremes may also be prepared by adjusting the concentration of the solution, the quantity, and the method of deposition and annealing.

Growth of Carbon Nanotubes by CVD. In Figure 2 are shown the morphologies of the carbon nanotubes produced by thermal CVD. Figure 2a shows the SEM images of the nanotubes from a low density of Ni nanoparticles. In comparison, Figure 2b shows the nanotubes grown with a higher catalyst loading, which yields a greater abundance of the tubes under identical CVD conditions, and indicates a strong relationship between the productivity and the catalyst loading. The tubes are, in general, uniform, and the diameter distribution falls in the range 20−30 nm. The tubes contain metal nanoparticles in the tip, suggesting the possible tip growth mechanism. The higher magnification images reveal that the morphology and quality of the tubes obtained at the higher catalyst density are very much similar to those obtained at the lower one, suggesting that the increase of the productivity takes place without sacrifice of the tube quality. Laser Raman examination (Figure 3) gives the feature of the multiwalled carbon nanotubes, with the D peak centered at 1360 cm^{-1} and the G peak at 1603 cm^{-1}.

Growth of Carbon Nanotubes by PECVD. A SEM image of the PECVD nanotubes is shown in Figure 4. It is seen that the abundant, vertically aligned carbon nanotubes cover most of the substrate surface. The image at a higher magnification

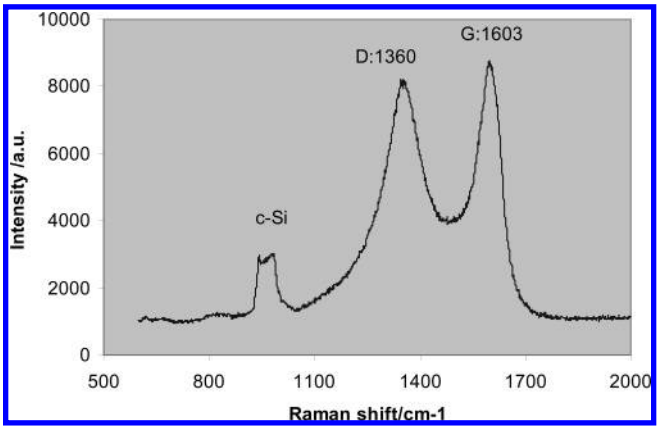

Figure 3. Raman profile of the CVD nanotubes showing the graphitic structure of the tubes (G peak) and the structural defect (D peak). The test was carried out using an Ar ion laser at $\lambda = 514.5$ nm.

reveals that the Ni nanoparticles are sitting at the tube tips, indicating the tip growth mechanism. Examination by laser Raman spectroscopy indicates the graphitic structure, with the characteristic G and D scattering peaks centered at 1600 and 1375 cm^{-1}, respectively. TEM observation was carried out because the SEM images did not provide significant information about the sidewalls of those vertically aligned tubes. The result shows that the nanotubes are multiwalled and most of them have an inner diameter of about 3−6 nm. This implies that most of the Ni nanoparticles are ca. 3−6 nm in size. Although defects or dislocations are frequently observed in the graphitic structure, the tubes are, in general, well crystallized in terms of the concentric graphene layers. Many tubes also contain a Ni particle encapsulated in the cavity. One of the encapsulated examples

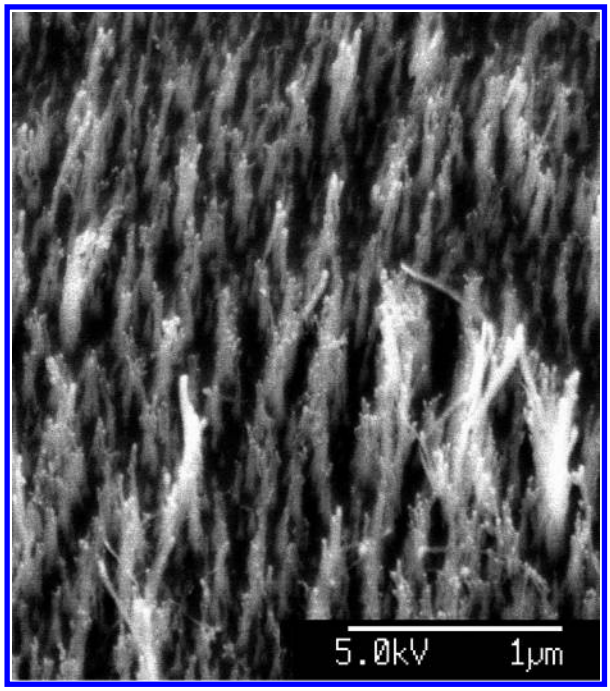

Figure 4. Vertically grown carbon nanotubes on the SiO_2/Si substrate by the plasma-enhanced CVD method using Ni nanoparticles as catalyst. The growth was conducted at 460 °C, with 1.1 mbar of NH_3 (100 sccm) and C_2H_2 (55 sccm).

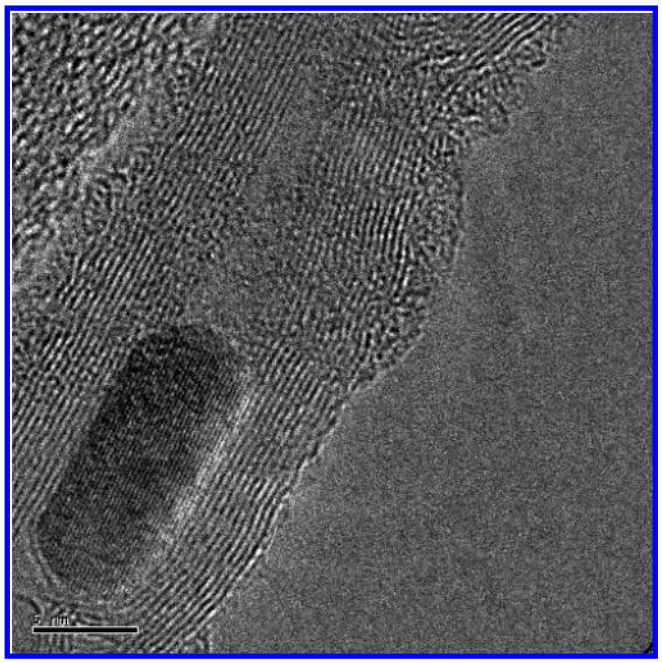

Figure 5. HRTEM image of a carbon nanotube vertically grown by the PEVCD method. This image shows the crystal fringes of the encapsulated nickel single crystal and the graphene layers. Using the graphene layers ($d = 0.344$ nm) as a reference, the fringe spacing of the metal is measured as 0.203 nm, corresponding to Ni(111) plane.

is shown in Figure 5. In this case, the metal nanoparticle is elongated along the tube axis. Using the graphene layers ($d = 0.344$ nm) as a reference, we measured the fringe spacing of the encapsulated metal particle at 0.203 nm, corresponding to the Ni(111) crystallographic facet. This image unambiguously indicates that the Ni particle is a pure single crystal, as evidenced by the lack of grain boundaries within the particle.

Discussion. The effectiveness of the CNTs growth in this work is mainly attributed to the highly active Ni nanoparticles formed from the formate precursor. First, we believe that among the many factors, the relatively low temperature of dissociation of the precursor has played an important role. Apart from the result presented in this paper, this characteristic may also be understood from other investigations. Nickel formate has been used as a precursor to metallic nickel in the preparation of nickel tetracarbonyl,[16] where the requirement of the purity of the formed metal is extremely high. In the area of so-called thick-technology, this compound has been used to study the formation of ideally spherical, agglomeration-free Ni particles at micrometer scale for applications in hybrid electronic products such as ceramic capacitor and batteries.[19,20] In those studies, nickel is replacing noble metals such as Pt, Pd, Ag, and Au, for use as electrode and thick-film material because of its good conductivity and lower cost. Xia et al.[21] have employed nickel formate as a precursor to produce micrometer scale Ni particles by an ultrasonic spray pyrolysis technique. They conclude that phase-pure nickel can be obtained at temperatures as low as 350 °C by the thermal decomposition of the precursor, which is the lowest temperature compared with using other nickel salts in the spray pyrolysis. They also find that nickel can be obtained at a residence time as short as 0.1 s at 600 °C, which is 1−2 orders of magnitude smaller than the times reported earlier using $Ni(NO_3)_2$ and $NiCl_2$ (1−100 s). Stopic et al.[22] have reported the effect of nickel formate on the decomposition temperature of dehydrated $NiCl_2$ in their differential thermal analysis (DTA) studies. DTA curves reveal that the reduction of the dehydrated $NiCl_2$ by hydrogen starts at 375 °C. While in the presence of a small amount of nickel formate (equivalent to 0.1 wt % Ni), this temperature drops to 275 °C, which matches the starting decomposition temperature of nickel formate. In comparison, our results indicate that much smaller Ni particles (1−30 nm) can also be formed from nickel formate for growth of carbon nanotubes.

In addition, the decomposition of nickel formate tends to produce Ni nanoparticles at a narrow size distribution. This may be seen from the AFM measurements and the growth results. In calcinations, it appears that the rapidly formed small nanoparticles (≤3 nm) at short calcination times and lower temperatures (e.g., ≤2 min at 500 °C) tend to adsorb some other species around them. This is particularly the case when a trace amount of surfactant with a long carbon chain, such as lauric acid, was mixed into the formate solution. This observation allows us to speculate that in the formate-derived Ni nanoparticles, some carbon-containing species formed from the thermal decomposition of the precursor might have helped to passivate the newly formed Ni particles from agglomeration, at least at the early stage of the nucleation of the particles.

Besides the temperature and size effects, the geometry of the particles is another factor in the determination of the growth behavior. In this work, at the growth temperatures, 530−545 °C for CVD and 460 °C for PECVD, the Ni particles (3−30 nm) are thought to be in solid state (compared with the melting point of the bulk nickel at 1455 °C). For the solid-state particles, they do not necessarily take a spherical shape. Instead, nanoparticles with mixed geometries were formed. This geometrical effect may not be particularly essential for growth of multiwalled nanotubes, as the produced Ni particles are relatively large (e.g., 5−30 nm), causing the intake and precipitation of carbon atoms to occur at a larger area of the grain boundaries or stage edges. Also, the normally found tip-growth mechanism allows the change of the shape of the particles during the growth procedure.[5] However, for growth of single-wall nanotubes, the Ni nanoparticles are required to be extremely small (1−3 nm)

and the nanotubes normally nucleate from the substrate-anchored particles by the base growth mechanism.[23] This situation makes only a small surface part of a nanoparticle exposed to the gas phase and hence very limited surface area is available for carbon uptake at the gas−nanoparticles interface. In this case, the geometry factor becomes more important. Gordon et al. have studied small Ni nanoparticles with atomic numbers particularly between 55 and 147 corresponding to a particle size of 1.0 and 1.5 nm, respectively.[24,25] In comparison of two geometrical configurations, cubooctahedra or icosahedra, they conclude that the cohesive energy between the nanoparticles of the same size and different geometry is very small ($\Delta E \leq 500$ cal/mol), indicating that the coexistence of both structures is possible. Considering the catalysis process in the growth of single-wall nanotubes, it is reasonable to assume that both structures would assist the nucleation of the tubes but lead to different tube structures or chiralities. The geometrical difference of metal particles may be a main responsible reason of why single-walled nanotubes obtained from a catalyst precursor route in CVD are always mixed in structure, even though the tube diameter may be controlled within a narrow range.

Conclusions

In this paper we have presented the following results. (1) Nickel formate serves as an ideal precursor for formation of Ni nanoparticles with a controllable size and a narrow size distribution. These freshly formed nanoparticles are catalytically very active, leading to a highly efficient growth of carbon nanotubes. (2) Growth of randomly distributed and vertically aligned carbon nanotubes on flat surface can be realized by either CVD or PECVD using the nickel formate route. As our method of deposition of the catalyst is solution-based, it has the merits of low-cost, ease of operation, large-area growth, and suitability for coating 3D substrates with complex shapes and structures. (3) The reason nickel formate is an ideal catalyst precursor is analyzed from a chemistry point of view. The self-redox feature of the decomposition reaction, together with the relatively low decomposition temperature (230−260 °C), distinguishes nickel formate from other common nickel precursors. In the case of nickel formate, it is not necessary to have external reducing agents such as H_2 for formation of the desired Ni nanoparticles. (4) The formed Ni nanoparticles can be nearly monodispersed in size, possibly arising from a tendency of the newly formed nanoparticles to chemically adsorb a thin layer of carbon-containing species produced from the precursor. This protective layer may passivate the particles from agglomeration particularly at the early stage of nucleation. (5) Although the particles size may be controlled within a narrow range, different geometrical structures coexist. We believe that this structural difference of metal leads to the structural difference of nanotubes, particularly in the case of growth of single-wall carbon nanotubes.

Acknowledgment. We thank financial support from Thomas Swan Co. & Lt., U.K., and the EU project CARDECOM GRD1-2001-41830. We also thank Dr. Ian A. Kinloch, Professor Alan H. Windle and Dr. Yali Li (Department of Materials Science, University of Cambridge), Mr. Stephen Cash and Dr. Charanjeet Singh (Thomas Swan Co. & Ltd., UK), and Dr. Milo S. P. Shaffer (Department of Chemistry, Imperial College, London) for helpful discussions.

References and Notes

(1) Baughman, R. H.; Zakhidov, A. A.; de Heer, W. A. *Science* **2002**, *297*, 787.

(2) Dresselhaus, M. S.; Dresselhaus, G.; Eklund, P. C. *Science of Fullerenes and Carbon Nanotubes*; Academic Press: San Diego, 1996.

(3) Ural, A.; Li, Y.; Dai, H. *Appl. Phys. Lett.* **2002**, *81*, 3464.

(4) Ren, Z. F.; Huang, Z. P.; Xu, J. W.; Wang, J. H.; Bush, P.; Siegal, M. P.; Provencio, P. N. *Science* **1998**, *282*, 1105.

(5) Helveg, S.; Lopez-Cartes, C.; Sehested, J.; Hansen, P. L.; Clausen, B. S.; Rostrup-Nielsen, J. R.; Abild-Pedersen, F.; Norskov, J. K. *Nature* **2004**, *427*, 426.

(6) Chhowalla, M.; Ducati, C.; Reppesinghe, N. L.; Teo, K. B. K.; Amaratunga, G. A. J. *Appl. Phys. Lett.* **2001**, *79*, 2079.

(7) Hofmann, S.; Ducati, C.; Kleinsorge, B.; Robertson, J. *Appl. Phys. Lett.* **2003**, *83*, 4661.

(8) Kleinsorge, B.; Golovko, V. B.; Hofmann, S.; Geng, J.; Jefferson, D.; Johnson, B. F. G. *ChemComm* **2004**, 1416.

(9) Ago, H.; Komatsu, T.; Ohshima, S.; Kuriki, Y.; Yumura, M. *Appl. Phys. Lett.* **2000**, *77*, 79.

(10) Edwards, A. B.; Garner, C. D.; Roberts, K. J. *J. Phys. Chem. B* **1997**, *101*, 20.

(11) Emmenegger, C.; Bonard, J. M.; Mauron, P.; Sudan, P.; Lepora, A.; Grobety, B.; Zuttel, A.; Schlapbach, L. *Carbon* **2003**, *41*, 539.

(12) (a) Geng, J.; Singh, C.; Shephard, D. S.; Shaffer, M. S. P.; Johnson, B. F. G.; Windle, A. H. *ChemComm* **2002**, 2666. (b) U.K. patent application No. 0216654.4.

(13) Choi, Y. S.; Cho, Y. S.; Kang, J. H.; Kim, Y. J.; Kim, I. H.; Park, S. H.; Lee, H. W.; Hwang, S. Y.; Lee, S. J.; Lee, C. G.; Oh, T. S.; Choi, J. S.; Kang, S. K.; Kim, J. M. *Appl. Phys. Lett.* **2003**, *82*, 3565.

(14) Niu, C.; Sichel, E. K.; Hoch, R.; Moy, D.; Tennent, H. *Appl. Phys. Lett.* **1997**, *70*, 1480.

(15) Hofmann, S.; Ducati, C.; Robertson, J.; Kleinsorge, B. *Appl. Phys. Lett.* **2003**, *83*, 135.

(16) Gilliland, W. L.; Blanchard, A. A. In *Inorganic Syntheses*; Fernelius, W. C., et al., Eds.; McGraw-Hill Book Co. Inc.: New York, 1946; Vol. II, Chapter 75, pp 234.

(17) *The Merck Index*, 13th ed.; Merck Research Laboratory, Division of Merck & Co.: Whitehouse Station, NJ, 2001; p 1166.

(18) Edwards, A. B.; Garner, C. D.; Roberts, K. J. *J. Phys. Chem. B* **1997**, *101*, 20.

(19) Messing, G. L.; Zhang, S. C.; Jayanthi, G. V. *J. Am. Ceram. Soc.* **1993**, *76*, 2707.

(20) Patil, P. S. *Mater. Chem. Phys.* **1999**, *59*, 185.

(21) Xia, B.; Lenggoro, I. W.; Okuyama, K. *J. Am. Ceram. Soc*. **2001**, *84*, 1425.

(22) Stopic, S.; Nedeljkovic, J.; Rakocevic, Z.; Uskokovic, D. *J. Mater. Res.* **1999**, *14*, 3059.

(23) Li, Y.; Kim, W.; Zhang, Y.; Rolandi, M.; Wang, D.; Dai, H. *J. Phys. Chem. B* **2001**, *105*, 11424.

(24) Gordon, M. B.; Cyrot-Lackmann, F.; Desjonqueres, M. C. *Surf. Sci.* **1977**, *68*, 359.

(25) Gordon, M. B.; Cyrot-Lackmann, F.; Desjonqueres, M. C. *Surf. Sci*. **1979**, *80*, 159.